Soft Matter

Accepted Manuscript

ROYAL SOCIETY OF CHEMISTRY

www.rsc.org/softmatter

Soft Matter

ARTICLE

Cell-sized liposome doublets reveal active tension build-up driven by acto-myosin dynamics

Received 00th January 20xx,
Accepted 00th January 20xx

DOI: 10.1039/x0xx00000x

www.rsc.org/

V. Caorsi†[a, b], J.Lemière†[a,b,c,d], C.Campillo[e], M.Bussonnier[a,b,c], J.Manzi[a,b], T. Betz[a,b,f], J.Plastino[a,b], K.Carvalho[a,b*] & C.Sykes[a,b]

Cells modulate their shape to fulfill specific functions, mediated by the cell cortex, a thin actin shell bound to the plasma membrane. Myosin motor activity, together with actin dynamics, contributes to cortical tension. Here, we examine the individual contributions of actin polymerization and myosin activity to tension increase with a non-invasive method. Cell-sized liposome doublets are covered with either a stabilized actin cortex of preformed actin filaments, or a dynamic branched actin network polymerizing at the membrane. The addition of myosin II minifilaments in both cases triggers a change in doublet shape that is unambiguously related to a tension increase. Preformed actin filaments allow us to evaluate the effect of myosin alone, while with dynamic actin cortices, we examine the synergy of actin polymerization and myosin motors in driving shape changes. Our assay paves the way for a quantification of tension changes triggered by various actin-associated proteins in a cell-sized system.

1 Introduction

The acto-myosin cortex is a contractile sub-micrometer thick actin network linked to the plasma membrane and containing myosin motors[1,2]. The cortex drives cell-shape changes, such as the ones occurring during division or in motility, and governs cell polarization[3] and tissue remodeling[3-6]. Cell behaviour depends on overall cell tension, a combination of the tension in the membrane, "membrane tension" and the tension in the cortex, "cortical tension", which is modulated by actin network organization and myosin motor activity[7-13]. Via its contribution to cell tension, acto-myosin dynamics modulates cell-cell adhesion as shown for cell doublets[14], a mechanism that is involved in cell sorting for tissue formation[15]. Recently, acto-myosin cortices have been reconstructed on supported lipid bilayers[16] and on cell-sized liposomes[17], allowing for an understanding of how actin filament crosslinking, cortex attachment to the membrane, and actin filament length, influence contraction by myosin and mechanical stress created by actin polymerization[18].

In this study, we use cell-sized liposome doublets to determine total tension changes produced by an acto-myosin cortex *in vitro*. Muscle myosin II is added to two different types of actin cortices: 1) a stabilized actin cortex composed of preformed actin filaments directly linked to the membrane (hereafter called "preformed filament" cortex); and, 2) a dynamic branched actin network polymerizing from the surface and linked to the membrane via an activator of actin polymerization (hereafter called "branched network" cortex). Variations in tension exerted by cortical activity alone are quantified by analyzing doublet-shape changes since membrane-membrane and membrane-cortex adhesion are kept constant. We find that preformed filament cortices do not induce an increase in tension except when myosin is added, hence allowing for the direct assessment of the contribution of myosin motors to tension production. In contrast, dynamic branched networks produce some tension build-up on their own that is further increased by the addition of myosin. Overall our assay allows for an evaluation of the role of myosin motors on tension build-up, either independently of actin dynamics or in synergy with branched network formation.

[a] *Laboratoire Physico Chimie Curie, Institut Curie, PSL Research University, CNRS, UMR168, 75005, Paris, France.*
[b] *Sorbonne Universités, UPMC Univ Paris 06, 75005, Paris, France.*
[c] *Univ Paris Diderot, Sorbonne Paris Cité, Paris, F-75205 France.*
[d] *Department of Molecular Biophysics and Biochemistry, Nanobiology Institute, Yale University, New Haven, CT, USA.*
[e] *Université Evry Val d'Essonne, LAMBE, Boulevard F Mitterrand, Evry 91025, France.*
[f] *Institute of Cell Biology, Center for Molecular Biology of Inflammation, Cells-in-Motion Cluster of Excellence, Münster University, Von-Esmarch-Strasse 56, D-48149 Münster, Germany*
** Current address: CytoDiag / BioPole Clermont-Limagne, Zi Zone de la Varenne, 63200 RIOM, France*

† These authors contributed equally to the work.
Electronic Supplementary Information (ESI) available: See
DOI: 10.1039/x0xx00000x

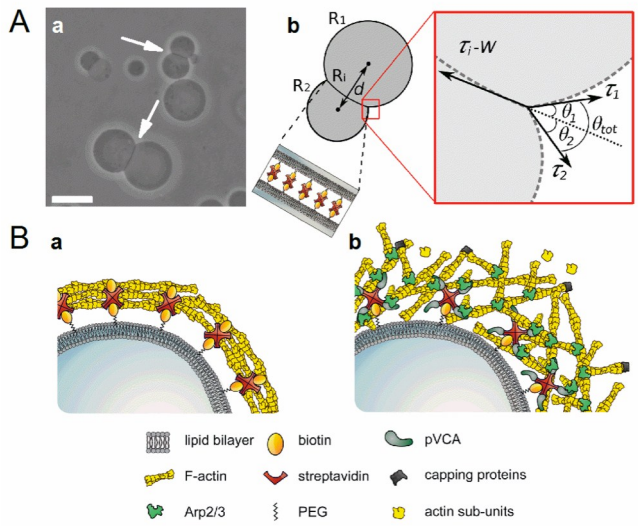

Fig 1. Cell-sized liposome doublets: geometry and different cortex systems. (Aa) Example of liposome doublets imaged by phase contrast microscopy, white arrows pointing at the interface. Scale bar, 10 µm. (Ab) Scheme showing geometrical parameters of the doublet. R_1, R_2 and R_i are respectively the radii of liposome *1*, liposome *2*, and the radius of the curvature of the interface between the two liposomes. Red inset: enlargement of the contact interface between the two liposomes showing tension vectors and contact angles. Black inset illustrating how liposome doublets are built via a biotin-streptavidin-biotin sandwich. (Ba) Drawing of preformed actin cortices obtained with preformed actin filaments bound at the membrane via a biotin-streptavidin link; proteins not to scale. (Bb) Drawing of branched network cortices obtained by the growth of a branched actin network activated by SpVCA proteins linked to biotinylated lipids at the membrane; proteins not to scale.

2 Results

2.1 Formation and analysis of liposome doublets

Liposome doublets are formed by addition of streptavidin in a solution of liposomes containing PEG-biotin lipids (**Fig 1Aa**). The geometrical parameters fully describing the liposome doublets are shown in **Fig 1Ab**: the distance between liposome centres (*d*), the radii of liposomes *1* and *2*, R_1 and R_2, respectively, the radius of curvature of the interface R_i and the angles between the interface and liposome *1* and *2*, θ_1 and θ_2, respectively. We define the total contact angle $\theta_{tot} = \theta_1 + \theta_2$.

Liposomes *1* and *2* have uniform surface tensions, τ_1 and τ_2. Tension refers to membrane tension in the absence of actin and myosin, and to the total contribution of membrane and cortical tension in their presence. The tension at the interface between liposome *1* and *2* reads $(\tau_i - W)$ with τ_i the interfacial tension and W the adhesion energy per unit surface due to biotin-streptavidin adhesion. For symmetrical doublets, formed by liposomes of similar radii (less than 25% difference in size) and a flat interface (see **Fig S1**) $\theta_1(t) = \theta_2(t) = \theta_{tot}(t)/2 = \theta(t)$. In these conditions, the Young's equation (see **Methods**) leads to the equality of tensions on both sides of the doublet, thus, $\tau_1(t) = \tau_2(t) = \tau(t)$ and we obtain

$$\tau_i - W = 2\tau(t).\cos\theta(t) \quad \textbf{(1)}$$

The effect of line tension at the contact line is negligible[19]. Note that **eq.1** is also valid for cell doublets and can be used to probe adhesion[15].

A reasonable assumption is that $\tau_i - W$ is constant over time for a given doublet (although it may vary from doublet to doublet depending on initial adhesion). The tension $\tau(t)$ varies over time because of actin polymerization and myosin activity; relative to its initial value $\tau_0(t)$, corresponding to the initial angle θ_0, reads:

$$\frac{\tau(t)}{\tau_0} = \frac{\cos\theta_0}{\cos\theta(t)} \quad \textbf{(2)}$$

In the following, as a preliminary step, we test if myosin activity on passive preformed filaments (**Fig 1Ba**) can lead to a significant change of θ, and thus tension. We indeed observe a visible effect, which prompted us to address, extensively and with statistical data, the more physiological case of a dynamic branched actin network (**Fig 1Bb**) in the presence of myosin motors.

2.2 Actin cortices with preformed filaments

Preformed actin cortices are obtained on doublets by adhering phalloidin-stabilized fluorescent actin filaments containing biotinylated actin monomers to the biotinylated liposome membrane via a streptavidin link (**Fig 1Ba and Fig 2Ba**). This gives a homogeneous shell, as already characterized on single liposomes[17]. The presence of this actin shell by itself does not modify the doublet shape. Indeed, ablating the actin network by photodamage[20] (and confirmed here by phase contrast microscopy observation in **Fig S2**) does not change significantly the shape of doublets, as observed by contact angle measurement (see **Fig 2A**, before (black symbols) and after (white symbols) complete photoablation of actin filaments). Myosin motors, preassembled into bipolar filaments around 0.7 µm long, are injected into the observation chamber by exchanging the external solution using an H-shaped flow chamber (see **Fig S3**). Addition of motors triggers a shape change of the doublets within minutes, and in 2D images (phase contrast and epifluorescence), we find that myosin addition produces an increase of contact angle. We measure a total contact angle θ_{tot} of (64±16)° (n=18) in the absence of myosin, whereas in the presence of 200 nM myosin we find a θ_{tot} value of (86±21)° (n=5). This difference is statistically significant (p=0.0186).

To permit the assumption leading to **equation 2**, $\theta_1(t) = \theta_2(t) = \theta(t)$, and to obtain an actual estimate of tension increase upon addition of myosin, only doublets with similar liposome size and showing a flat interface are considered. For this purpose, 3D spinning disk image stacks are recorded in the presence of sulforhodamine B (SRB) in one of the liposomes, to better visualize the interface (see **Fig S1**). We also use a lower myosin concentration (50nM) to increase the observation time after myosin addition and before symmetry breaking: as reported in [17], increasing myosin concentration accelerates tension build-up and thus decreases the time to cortex rupture.

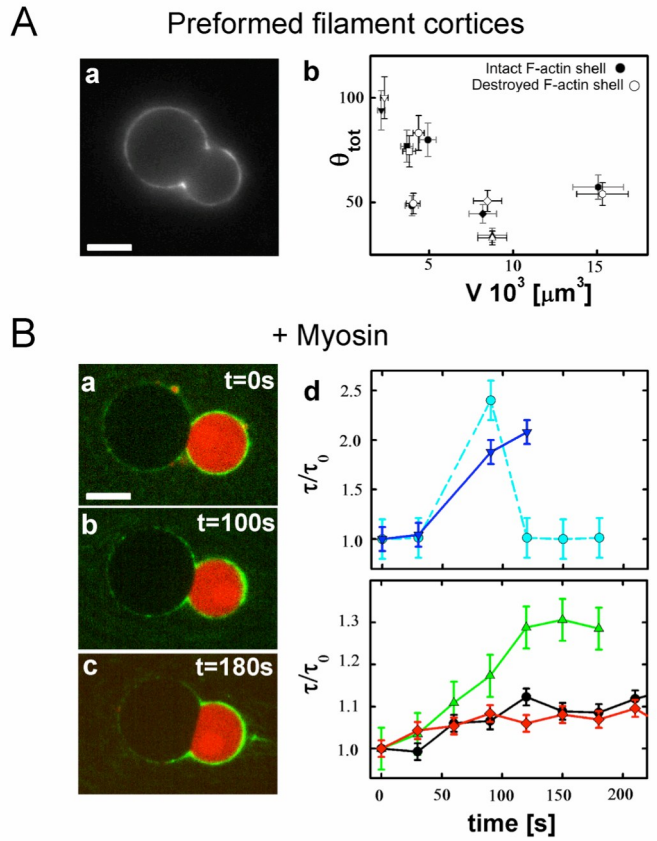

Fig 2. Doublet shape changes in preformed filament cortices in the absence (A) or presence (B) of myosin. (Aa) Epifluorescent image of a doublet with a preformed filament cortex. (Ab) Total contact angle before (white symbols) and after (black symbols) complete ablation of the actin cortex for different doublets volumes, showing no significant effect of the addition of preformed actin filaments on doublets shape (angle difference of 3.4±2°, n=7). (B) Effect of 50 nM myosin on doublet shape. (Ba-c) Spinning disk images of a doublet before (Ba) and after myosin injection (Bb) and (Bc) (see **supplemental Video S1 and Video S2**) The actin cortex is labeled in green (Alexa488-actin fluorescence, 10% of total actin); one liposome contains SRB (sulforhodamine B) in red to visualize the interface of the doublet; scale bar is 5 µm. (Bd) Tension increase over time normalized by τ_0 the initial value before injection of myosin (final concentration of 50 nM) for five different doublets displayed in two graphs for clarity. Each color represents a doublet recorded in a different set of experiment; the red curve corresponds to images displayed in (Ba-c). The blue dashed line corresponds to a case where actin cortex rupture occurs, showing recovery of initial tension value. Error bars represent measurement accuracy (see **Methods**).

A contact angle increase as a function of time upon 50nM myosin addition is observed (**Fig 2Ba-c**), as well as a decrease in distance *d* between the liposome centres at constant volume (**supplemental Fig S4**, **Video S1 and Video S2**). The corresponding relative tension increase is shown in **Fig 2Bd**. Conversely, the angle, and therefore the tension, decreases when the preformed actin cortex, in the presence of myosin motors, is ablated (**Fig S5** and **supplementary Video S55**).

2.3 Actin cortices with branched network

In order to more closely approximate a cell cortex, a polymerizing branched network is formed on liposome doublets. The Arp2/3 complex is activated at the membrane via streptavidin-pVCA, henceforth named S-pVCA (VCA is the domain of WASP that recruits and activates the Arp2/3 complex) grafted to the membrane (see **Methods**, **Fig 1Bb** and [18]). Fine-tuning in protein amounts (actin, profilin, the Arp2/3 complex and capping protein (CP)) is needed to produce an appropriate actin shell, sufficiently thick and cohesive to allow myosin contraction, but yet thin enough to prevent symmetry breaking by actin polymerization alone and with a thickness ten times smaller than the average liposome radius, so as to be considered as a sheet in the shape of a shell and not a 3D bulk network (**Fig S6,** [20,21]). In addition, the actin shell must be homogeneous to avoid immediate symmetry breaking upon myosin addition[18]. At a profilin/actin ratio of 1:1, reactions containing 35nM Arp2/3 and 20 nM CP give a thin homogeneous actin shell that grows to saturation within an hour (**Fig 3Aa** and inset **b, c** and **d** showing example of doublets imaged at 10 min, 25 min and 45 min respectively; see **Fig S7** for actin shell thickness).

To optimize data collection, we estimate the angle in a large population of doublets under the same experimental conditions. To avoid inaccuracy in angle measurements in projected images, since doublets do not have their long axis necessarily parallel to the image plane, we measure the interface length *PQ* and the liposome radius *R* ($R=R_1=R_2$) by z-tuning in phase contrast images to achieve the largest values. The distribution of the angle θ is then obtained through $PQ = 2R\ sin\,\theta(t)$ (**Fig 3Ae and 3Af**). A shift towards higher values of θ is observed at longer actin polymerization times, consistent with stress build-up produced by growing actin shells in this geometry[22,18].

Adding 20 nM of myosin at different times after mixing the doublets with the actin polymerization mix (specifically at 15 min at 30 min and at 60 min of actin polymerization) leads to a further shift towards higher angles compared to actin alone (**Fig 3Bf and inset**), thus highlighting the cooperative work of actin polymerization and myosin motors in driving shape changes. To observe this effect in real time on a single doublet, we use a micropipette aspiration set-up to immobilize doublets and thus have access to the time course of doublet shape changes upon addition of myosin motors to a branched actin network (**Fig 3Ba-e and supplementary Video S3**). As already observed for preformed actin filaments, an increase in contact angle of the doublet is observed, demonstrating an increase in tension upon myosin addition (**Fig 3Bf and inset**).

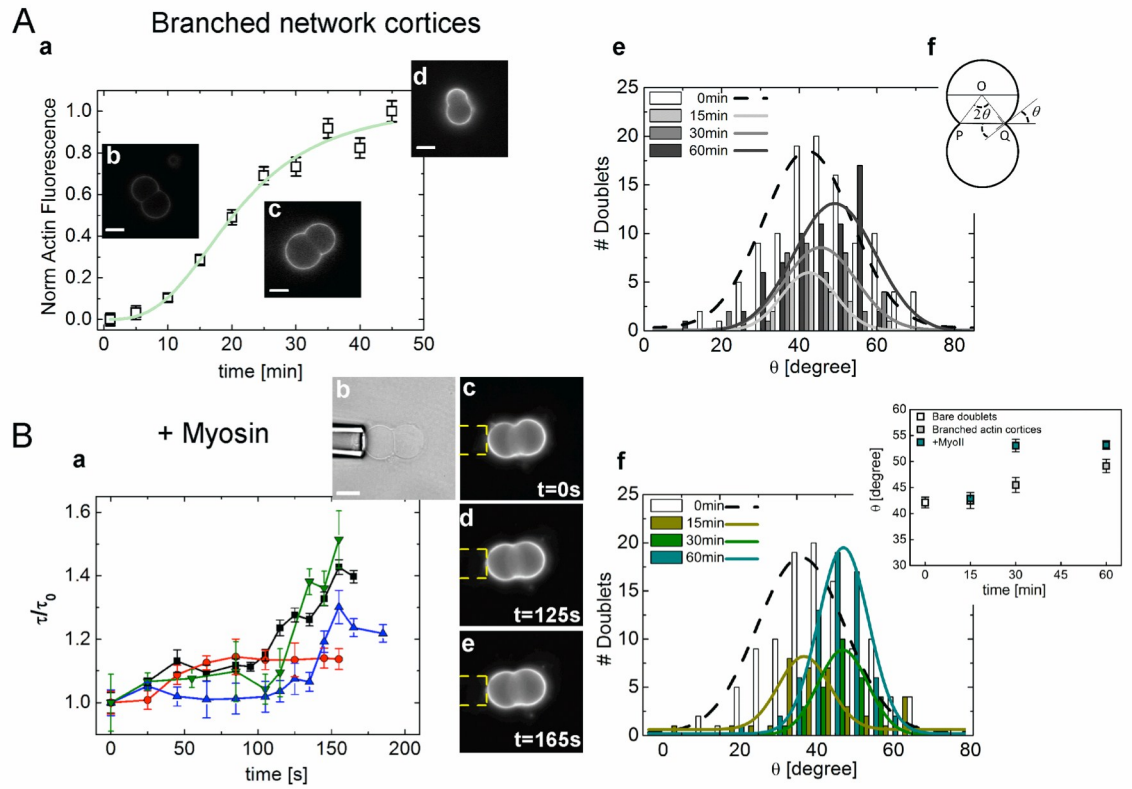

Fig 3. Doublet shape changes in branched network cortices in the absence (A) or presence (B) of myosin. (Aa) Normalized actin fluorescence increase as a function of time and three representative images for (Ab) 10 min, (Ac) 25 min and (Ad) 45 min after adding the actin polymerization mix. (Ae) Shift of the peak of contact angle distributions measured from interface length PQ (scheme Af) for bare doublets (0min, n=109), and at different times after the actin polymerization mix is added: at 15 min (n=21), 30 min (n=40) and 60 min (n=66). (B) Effect of myosin on branched network cortices. (Ba) Time evolution of tension ratio upon myosin addition (t=0 min) after 30min of polymerization in single doublets held in place with the use of a micropipette (each doublet is represented by a different line color, each recorded in a different set of experiment). (Bb-e) Images corresponding to black curve of (Ba) and **supplemental Video S3**. (Bb) Bright field image of a doublet held in a micropipette. (Bc-e) Epifluorescent images of the same doublet before (Bc) and after addition of myosin (Bd) and (Be). (Bf) Shift of the peak of contact angle distributions at different times after actin polymerization initiation (15 min, n=36; 30 min, n=29; 60 min, n=67), images were taken 2-15 minutes after myosin addition. For this experiment, similarity criterion for liposome size in doublets was reduced to 15%. (3Ae) and (3Bf) correspond to two or three different independent experiments repeated in the same conditions, data are available in **SourceData-Fig3Ae-3Bf.xlsx**. Inset: Contact angle (mean ± SEM) as a function of time in only actin polymerization conditions (grey symbols) and upon addition of myosin (green symbols). No significant difference (Student T-test) is observed upon addition of myosin at 15min, while there is a significant difference at 30 min and at 60 min after myosin addition (p=0.0029 and p=0.0004 respectively). Scale bars are 10 µm.

2.4 Measurement of membrane tension of bare doublets

Because **equation (2)** only allows for an evaluation of a relative change of tension, it is important to know the initial tension of a bare liposome doublet. Membrane tension of single liposomes (prior to doublet formation), and liposome doublets is measured by recording membrane fluctuations with a weak (low power) optical tweezer system (see **Methods** and [23]) (**Fig 4Aa**). Briefly, 3 to 4 beads are used to keep the doublet/liposome suspended on a glass surface, covered with PLL-PEG to avoid surface attachment, while a laser probe at low power (0.5mW) is used to scan and detect membrane fluctuations and derive membrane tension (**Fig 4A**). Strikingly, we do not observe a significant difference in tension between liposomes and doublets, suggesting that the liposome volume changes during the adhesion process. Average values are $1.2\pm0.9\times10^{-6}$ N/m for bare liposomes and $1.1\pm0.8\times10^{-6}$ N/m for doublets (average ± SDT), as can be seen in **Fig 4A**. The observed data dispersion is in agreement with literature values [24-26].

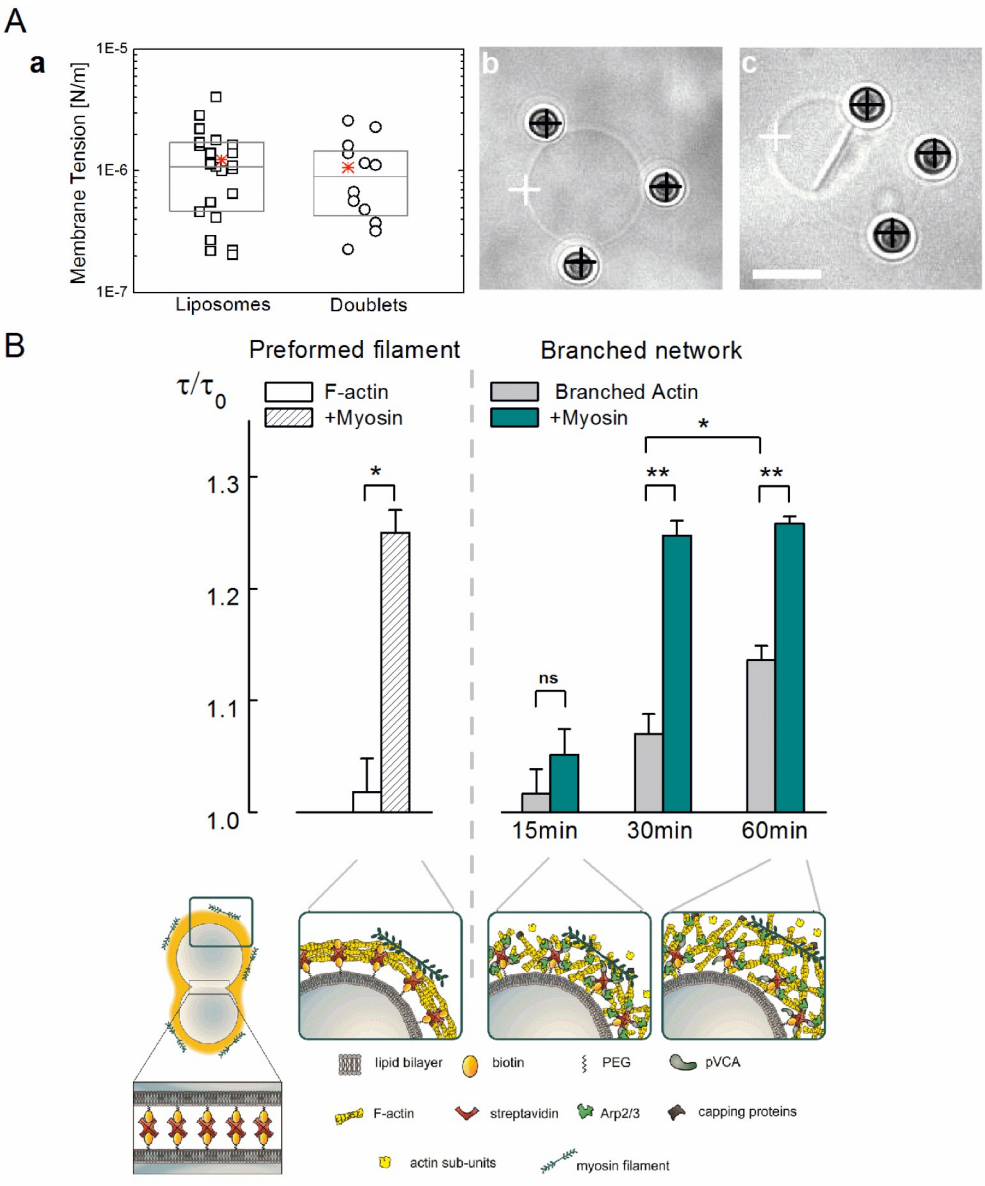

Fig 4. Absolute tension values for bare liposomes and tension increase by myosin addition for both preformed filament and branched network cortices (schemes at the bottom highlight experimental conditions).
(A) Membrane tension measured by time resolved membrane fluctuation spectroscopy[23]. (Aa) Membrane tension values, box plot represents percentiles (25%, 50%, 75%), red star is the average value (liposomes n=22, doublets n=12, five independent experiments repeated in the same conditions, see **supplemental Fig S9** and data available in **SourceData-Fig4A.xlsx**). (Ab, c) Bright field image examples of a single liposome (Ab) and a doublet (Ac) held with three beads trapped by multiple optical tweezers. The white cross represents the position of the fluctuation scan laser beam. Black crosses help to locate traps at the beginning of the experiment. Scale bars, 10 µm. (B) For preformed filament cortices, tension increase is estimated by measuring the angle on 2D projected images (n=5) whereas on branched network cortices, tension increase is estimated by the statistical analysis presented in **Fig 3Ae** and **3Bf** (see legend of **Fig 3** for sample size). In all cases the normalized tension increases upon myosin addition (dashed bar compared to white bar, and green bars compared to grey bars). In the case of branched network cortices that grow over time at the liposome surface, there is an increase in tension even in the absence of myosin (compare the 3 grey bars) related to the cortex thickening (see scheme and **Fig S7**). Bars represent average values ± SEM. ns: non-significant difference; * $p<0.01$; ** $p<0.005$.

2.5 Relative tension increase in preformed and branched actin network cortices

Both preformed actin filament cortices and branched network cortices display an increase in tension upon addition of myosin. Note that the relative tension increase for preformed filament and branched filament cortices seem to be similar, consistent with previous observed critical tensions for cortex rupture which were found to be similar in both conditions[18]. However, a striking difference is that a preformed actin cortex, in the absence of myosin, does not affect doublet shape while branched network cortices do, with a significant effect at 30 minutes of polymerization. At this time of 30 minutes, before myosin is added, the branched network cortex is indeed already under tension, or pre-stressed, being still active at 60 minutes and building up tension by continuous polymerization (grey bars on the right of **Fig 4B**). At 15 minutes the network is not yet cohesive enough to induce sufficient pre-stress and to allow myosin motors to bind and contract the network, thus leading to a non significant increase of tension at this time (**Fig 4B**). Further, we observe that addition of myosin on an already pre-stressed actin network does not change the tension when pre-stress is increased, at 60 minutes compared to 30 minutes (same height of two right green bars on **Fig 4B**). Note that under our experimental conditions, after 60 minutes of actin polymerization on its own without myosin addition, symmetry breaking occurs, i.e., cortex ruptures and relaxes liposome shapes. Our data show that pre-stress produced by actin polymerization modifies the amount of stress that can be produced by myosin motors addition.

3 Discussion

Interaction of myosin motors with a biomimetic actin cortex induces tension build-up in cortices made of preformed unbranched filaments or dynamic branched networks, as can be observed in **Fig 2B**, **Fig 3B** and **Fig 4**. The tension, normalized to its initial value, increases and reaches maximal values τ_{max} that are in the range of 1.3 τ_0 but can attain values of 2.3 τ_0. Higher values lead to cortex breakage where the doublet recovers its initial shape before myosin addition (see blue dashed line in **Fig 2Bd**). Myosin-induced shape changes are also reversed by ablating the actin network, demonstrating that the increase in tension is indeed due to stresses in the acto-myosin cortex (**Fig S5 and Video S5**). The increase in tension by a factor of about 1.3 to 2.3, here obtained when myosin is added, mirrors the changes measured in cells when myosin activity is impaired in different cell types, either by drugs or by genetic manipulation: tension was observed to decrease by about two-fold in these cases[7,11,12,27]. Therefore, the small relative change in tension observed in our experiments upon addition of myosin motors is relevant compared to what is observed in cells.

Tension is also produced in our experimental set-up by actin polymerization alone (**Fig 4**), while doublet tension is unchanged by the presence of preformed filament cortices (**Fig 2Ab**). In fact, actin in cellular cortices is dynamic and continuously polymerizes from the membrane. Therefore, its role in cell tension needs to be taken into account, as confirmed by experiments demonstrating that cell tension drastically changes when actin dynamics are affected, for example when actin-filament severing proteins are impaired[7].

For branched network cortices, it has been shown previously that actin growth from a spherical surface generates a normal stress (inward pressure)[22]. This normal stress reads $\sigma_n = E(e/R)^2$ where E is the elastic modulus of the actin network, e the thickness of the cortex and R the radius of the liposome. The value of E depends on the mesh size that is estimated as 100 nm in our conditions[21], thus leading to a value of E on the order of 10^2 Pa, smaller than that reported in studies of actin comets, which have denser actin networks[28]. Taking e on the order of 600 nm (**Fig S7**) and R on the order of 5 µm, we estimate the inward pressure induced by the actin network pushing on the membrane in the order of 1 Pa. This normal stress results in a tangential stress at the outer boundaries of the actin shell that reads $\sigma_t = Ee/R$, with the same notation as above. This stress can be translated into tension $\tau_{bc} = \sigma_t e = Ee^2/R$, leading to an estimate value for $\tau_{bc} = 8\text{x}10^{-6}$ N/m.

How does this compare to the tension developed by myosin on its own? An upper estimate of cortical tension induced by myosin addition in both types of cortices in our study can be obtained as in [17] where the critical tension τ_c for cortex breakage (or "peeling") under myosin contraction was calculated as the ratio of the force generated by the motors to the characteristic size $2R$ of the liposome. An average of three myosin filaments already leads to cortex breakage[17] (**Supplementary Fig S8**). Each myosin minifilament is composed of a number N_m of ~100 motors with a duty cycle (DC) between 5% and 18% [29], each motor pulling with a force F_m of ~3.5 pN[30].. With a liposome size R of around 5 µm, we obtain an estimate of the tension $\tau_c = F_m N_m DC/2R$ between $5\text{x}10^{-6}$ N/m and $2\text{x}10^{-5}$ N/m. Note that this expression is valid for a cohesive network at high density of actin filaments where all myosin are in contact with a filament. This is a rough upper-bound estimate that is comparable to polymerization-induced tension. So as we also show experimentally in this study, actin polymerization contributes as much as myosin to tension production, although it remains to be seen if this is likewise true in cells where the geometry is different. In this context, it is important to note that both of these values are a few times larger than the membrane tension measured on bare doublets, on the order of 10^{-6} N/m. This is consistent with the increases of tension we observe in our experiments.

Importantly, we observe here that the effect of myosin on branched network cortices depends on actin network properties, echoing earlier studies: the addition of myosin after 15 minutes of polymerization does not lead to a significant increase in tension because the actin cortex is not yet cohesive enough to allow for efficient contraction by myosin motors (**Fig 4B**)[21]; moreover, addition of myosin to an already pre-stressed actin network does not change when pre-stress is increased (**Fig 4B**). This indicates that the network put under stress in these conditions cannot contract further, revealing that myosin motors maybe stalled by the pre-stressed network. This is the first time such an effect is evidenced since previous studies used geometries with free boundary conditions[31-34] that allows the actin network to relax. Here boundary conditions are fixed by the sphericity of our shell allowing a pre-stress in the network.

Tensions in our systems, including pure membrane tension, are smaller than tensions estimated in cells, where overall tensions range from $5x10^{-5}$ N/m in fibroblast progenitor cells[11] or dividing mouse oocytes[35], and up to $4x10^{-3}$ N/m for *Dictyostelium*[12]. Membrane tension in cells is found to be $(3.9\pm0.4)\ x10^{-5}$ N/m, higher than in lipid vesicles, as elegantly demonstrated by Tinevez and co-workers[7], in L929 cells. This discrepancy might be due to a residual tension contribution of erythrocytic-like cytoskeleton[7].

It is worth reminding that measurements in our system are limited by critical tensions before cortex ruptures which might be one of the limiting factor to reach higher levels of cortical tension. Furthermore, in cells, as well as in our system, cortical tension depends on the presence of protein regulating actin turnover such as depolymerizing factors (ADF-cofilin, gelsolin) which play an essential role in increasing/decreasing cortical tension. Formins as well would play an important role as the other most important contributors to cortical actin assembly (the other being Arp2/3)[36]. In fact, filaments produced by these two pathways differ completely in number, length and turnover kinetics[36]. As demonstrated in cell, despite that only 10% of cortical actin is due to formin, formin-originating-filament lengths are 10 times longer than Arp2/3-ones, and can bundle, thus highly contributing to cortical tension[36], a mechanism that will be addressed in the future.

Surely the two approaches, in vitro and in cells, are different: in our system we build cell tension brick by brick, in cells bricks can only be destroyed. Nonetheless they both have advantages and limitations, are complementary, and need to be pushed further in order to unveil the generic mechanism of tension build up in cells.

4 Conclusion

We provide a biomimetic reconstitution of tension build-up through acto-myosin contractility using liposome doublets carrying two types of actin cortices, either composed of preformed filaments or of dynamic branched networks. Tension is monitored *in situ* over time on single doublets, and on doublet populations, by analyzing changes in doublet shape. This method allows us to directly quantify the relative increase in tension due solely to myosin, separately from actin dynamics, or their dual contribution in tension build-up. More needs to be done in the future to understand tension build-up due to the combined activity of actin and myosin in a geometry that is closer to that of the cell, using encapsulation methods[37-40], with actin dynamics reproduced at the inner leaflet of the liposome[41]. Understanding contraction of composite systems built on the model of a cell paves the way for the reconstitution of complex systems like tissues.

5 Material and Methods

5.1 Lipids, reagents, proteins and buffers

Chemicals are purchased from Sigma Aldrich (St. Louis, MO, USA) unless specified otherwise. L-alpha-phosphatidylcholine (EPC) and 1,2-distearoyl-sn-glycero-3-phosphoethanolamine-N-[biotinyl polyethylene glycol 2000] (biotinylated lipids), are purchased from Avanti polar lipids (Alabaster, USA). Actin and biotinylated actin are purchased from Cytoskeleton (Denver, USA) and used with no further purification. Fluorescent Alexa-488 actin is obtained from Molecular Probes. Bovine Arp2/3 complex is purchased from Cytoskeleton and used with no further purification. Wild-type human profilin, mouse capping protein (CP) and His-pWA–streptavidin (S-pVCA) are purified as previously described[18]. Myosin II is purified from rabbit skeletal muscle as previously described[42] and its functionality is confirmed by motility assays showing an average gliding speed of 4.5 $\pm$ 1.5 µm/s (N = 27)[43]. Myosin II minifilaments (approximately 0.7 µm length with about 100 motors[42]) are preformed before injection into the experimental chamber. The G-Buffer contains 2mM Tris, 0.2mM $CaCl_2$, 0.2mM DTT at pH 8.0. The working buffer contains 25 mM imidazole, 50 mM KCl, 70 mM sucrose, 1mM Tris, 2 mM $MgCl_2$, 2 mM ATP, 0.1 mM DTT, 0.02 mg/ml β-casein, adjusted to pH 7.4. Osmolarity of the working buffer with and without myosin II are 220 mOsm within 5% error, as checked with an automatic osmometer (Loser Messtechnik).

5.2 Formation of liposome doublets

Liposomes are electroformed[44]. Briefly, 20 µL of a mixture of EPC lipids and biotin PEG lipids (molar ratio of 0.1% or 1%) with a concentration of 2.5 mg/ml in chloroform/methanol 5:3 (v:v) are spread on ITO-coated plates, dried under nitrogen flow, then placed under vacuum for 2 hours. A chamber is formed using the ITO plates (their conductive sides facing each other) filled with sucrose buffer (200 mM sucrose, 2 mM Tris adjusted at pH 7.4, containing or not sulforhodamine B 0.9 µM), and sealed with hematocrit paste (Vitrex medical, Denmark). Liposomes are formed by applying an alternate current voltage (1 V - 10 Hz) for 75 minutes. Then, liposomes are incubated with 160 nM streptavidin in non-saturating conditions of biotin sites (**Supplementary Fig S10**) for 15 min and diluted 30 times to remove unbound streptavidin from the solution. Note that for the observation of the interface between the doublet liposomes we prepare separately liposomes in the presence or in the absence of 0.9 mM sulforhodamine B, and mix them at equal volume before incubation with streptavidin. At this stage we have doublets coated with streptavidin. Waiting more than 15 min would increase the quantity of liposome aggregates and decrease the quantity of doublets and single liposomes.

5.3 Tension measurements on bare liposomes and liposome doublets

Membrane tension is measured by time resolved membrane fluctuation spectroscopy as previously described[23]. Briefly, membrane fluctuations are measured using the deflection of a weak laser off the liposome-buffer interface. To avoid drifting of the liposome during the measurement three to four beads (3 µm polystyrene beads, Polysciences Europe GmbH, Germany) are used to sterically fix the liposome in space. Beads are pre-treated with BSA (bovine serum albumin, Sigma-Aldrich) to avoid membrane adhesion. Each bead is trapped by an optical tweezer using an effective laser power of around 15-20 mW. The probe laser with a low power (typically 0.5-1 mW) allows for measuring membrane fluctuations, by specifically measuring the difference in refractive index at the membrane with a quadrant photodiode (QPD). As described in [23], we derive tension values from the fluctuation spectrum. Briefly, the Fourier transform of the time dependent membrane position is used to calculate the power spectral density (PSD) plot as a function of frequency (**Supplementary Fig S9**). Knowing the bending rigidity of the membrane used, the PSD depends mainly on the membrane tension. Fitting the theoretical PSD to the data[23] we can determine the membrane tension. Fitting quality is excellent (R^2> 0.9). To avoid high frequency shot noise as well as drifting noise from the instrument, the frequency range for the fitting is limited to 1-10^3Hz.

5.4 Actin cortices with preformed filament

As described in detail in[44], actin monomers (stock solution of 40 µM in G-buffer) containing 10% fluorescently labelled actin and 1/400 biotinylated actin monomers is polymerized at a final concentration of 1 µM in the working buffer for 1 hour in the presence of 1 µM of phalloidin (to prevent depolymerization). This solution is then diluted 10-fold to 0.1 µM actin, and incubated for 15 min with streptavidin-coated liposome doublets. The mix is diluted 5 times for observation to reduce background fluorescence of actin filaments.

5.5 Actin cortices with a branched network

Liposome doublets are first incubated with an activator of actin polymerization (S-pVCA, 350nM[18,21,45]) via a streptavidin-biotin link. Actin polymerization is triggered by diluting this first solution 10 times in a mix containing 3 µM monomeric actin (10% fluorescently labelled with AlexaFluor488), 3 µM profilin, 35 nM of the Arp2/3 complex and 20nM of CP, in the working buffer.

5.6 Observation of doublets

Observation in 2D: epifluorescence, phase contrast and bright-field microscopy are performed using an IX70 Olympus inverted microscope with a 100x or a 60x oil-immersion objective. Images are collected by a charge coupled device CCD camera (CoolSnap, Photometrics, Roper Scientific). Single doublet observation is done either by using chambers made as described in supplementary (**Fig S3**), or by holding the doublet in micropipettes. Micropipettes are fabricated by pulling borosilicate capillaries (0.7/1.0 mm inner/outer diameter, Kimble, Vineland, NJ) with a laser-based puller (P2000, Sutter Inst. Co, Novato, CA), and adjusted to the desired sized (6-8 µm) by using a microforge (MF-830, Marishige, Japan). To prevent adhesion of liposome doublets to the micropipette walls, pipettes are incubated in 0.1 mg/mL PolyEthyleneGlycol-PolyLysin (PLL(20)-g[3.5]-PEG(2), Surface Solution, Dubendorf Switzerland) in HEPES solution (pH 7.3) for 15 min. The observation chamber, made by a U-shaped Parafilm spacer (2 cm 2 cm 5 mm), sandwiched in between two microscope

slides, is placed on the stage of the microscope. The aspiration pressure is adjusted by controlling the height (0.25 mm) of a mobile water tank connected to the micropipette. This gentle aspiration is sufficient to hold doublets covered with branched-network cortices during addition of myosin and avoid doublet displacement. Right after myosin addition, the aspiration pressure is put to zero for doublet observation.

Observation in 3D: spinning-disk confocal microscopy is performed on a Nikon Eclipse T1 microscope with an Andor Evolution Spinning Disc system and a 60x water immersion objective and a z distance between z-slices of 1/25 of the doublet size.

5.7 Analysis of doublet shape

Young's equation, which relates tensions and angles, can be applied to the contact line between the two doublet liposomes (**Fig 1A, right**). When projected on the tangent to the interface between liposomes, Young's equation reads:

$$\tau_i - W = \tau_1 \cos\theta_1 + \tau_2 \cos\theta_2 \qquad \textbf{\textit{(m1)}}$$

When projected orthogonally to the contact surface tangent, one finds:

$$\tau_1 \sin\theta_1 = \tau_2 \sin\theta_2 \qquad \textbf{\textit{(m2)}}$$

2D-images: Two circles are adjusted on doublet contours on binarized images taken by phase contrast or epifluorescence microscopy using ImageJ. Obtained shape descriptors are: contact angle, interface length, diameter of each doublet liposomes 1 and 2. For the statistical analysis, angle distributions are fitted with a Gaussian. A Welch's t-test (two-sample T-test with no equal variances) is used to evaluate statistically significant differences.

3D-images: the geometrical parameters of the doublets are determined by optimizing the correlation between simulated and acquired 3D recording. Simulated 3D stacks, using [Python], [Numpy] and [Cython] are obtained by creating two spherical caps in contact and reproducing the fluorescent signal of actin at the external surface. Optimizing the correlation between simulated and acquired data is done using [Python] and [SciPy] (Nelder–Mead simplex method from the "optimize" submodule). Initial fit parameters of the first frame of each time lapse are determined visually. For the subsequent frame, we use the optimized parameters as initial parameters. Robustness of fit is checked by several repeats while changing the initial fit parameters by a random amount drawn from a normal distribution (mean 0 µm and standard deviation 0.5 µm). The obtained eight parameters (2 centers with X,Y,Z coordinate and 2 liposomes radii) geometrically define the contact angle and the distance between centers. All the data processing was done in an [IPython] environment.

All values are reported as average+/- SDT except when noted otherwise.

Acknowledgements

This work was supported by the French Agence Nationale pour la Recherche (ANR), grant ANR 09BLAN0283, ANR 12BSV5001401 and ANR-11-JSV5-0002, and by the Fondation pour la Recherche Médicale (FRM), grant DEQ20120323737. We thank Dr Agnieszka Kawska at IlluScientia for schemes. JL and MB thank the AXA Research Fund for doctoral fellowships. JL and KC were also supported by la Fondation ARC pour la recherche sur le cancer. We thank Wylie Ahmed and Fabrice Valentino for help with the optical tweezer setup, Raphaël Voituriez and Enrique de la Cruz for very enlightening discussions and Thomas Risler for critical reading of the manuscript.

References

1. Clark AG, Dierkes K, Paluch E. Monitoring Actin Cortex Thickness in Live Cells. *Biophys. J.* 2013; **105** (3): 570-580.

2. Salbreux G, Charras G, Paluch E. Actin cortex mechanics and cellular morphogenesis. *Trends Cell Biol.* 2012; **22**(10): 536-45. doi: 10.1016/j.tcb.2012.07.001.

3. Munro E, Nance J, Priess JR. Cortical flows powered by asymmetrical contraction transport PAR proteins to establish and maintain anterior-posterior polarity in the early C. elegans embryo. *Dev. Cell* 2004; **7** (3): 413-424.

4. Lecuit T, Lenne P-F. Cell surface mechanics and the control of cell shape, tissue patterns and morphogenesis. *Nat. Rev. Mol. Cell Biol.* 2007; **8** (8): 633-644.

5. Rauzi M, Lenne P-F, Lecuit T. Planar polarized actomyosin contractile flows control epithelial junction remodelling. *Nature* 2010; **468** (7327): 1110-1114. doi: 10.1038/nature09566.

6. Rauzi M, Lenne P-F. Cortical forces in cell shape changes and tissue morphogenesis. *Curr. Top. Dev. Biol.* 2011; **95:** 93-144. doi: 10.1016/B978-0-12-385065-2.00004-9.

7. Tinevez J-Y, Schulze U, Salbreux G, Roensch J, Joanny J-F, Paluch E. Role of cortical tension in bleb growth. *Proc. Natl. Acad. Sci.* 2009;**106** (44): 18581-18586. doi: 10.1073/pnas.0903353106.

8. Nambiar R, McConnell RE, Tyska MJ. Control of cell membrane tension by myosin-I. *Proc Natl Acad Sci* 2009; **106** (29): 11972-11977. doi: 10.1073/pnas.0901641106.

9. Raucher D, Stauffer T, Chen W, Shen K, Guo S, York JD, Sheetz MP, Meyer T. Phosphatidylinositol 4,5-bisphosphate functions as a second messenger that regulates cytoskeleton-plasma membrane adhesion. *Cell* 2000;**100** (2): 221-228.

10. Sens P and Plastino J. Membrane tension and cytoskeleton organization in cell motility. *J. Phys.: Condens. Matter* 2015; **27:** 273103-13.

11. Krieg M, Arboleda-Estudillo Y, Puech P-H, Käfer J, Graner F, Müller DJ, Heisenberg C-P. Tensile forces govern germ-layer organization in zebrafish., *Nat. Cell Biol.* 2008; **10** (4): 429-436. doi: 10.1038/ncb1705.

12. Schwarz EC, Neuhaus EM, Kistler C, Henkel AW, Soldati T. Dictyostelium myosin IK is involved in the maintenance of cortical tension and affects motility and phagocytosis. *J. Cell Sci.* 2000;**113** (4): 621-633.

13. Luo T, Mohan K, Iglesias PA, Robinson DN. Molecular mechanisms of cellular mechanosensing. *Nat. Mater.* 2013;**12** (11):1064-1071.

14. Engl W, Arasi B, Yap LL, Thiery J-P, Viasnoff V. Actin dynamics modulate mechanosensitive immobilization of E-cadherin at adherens junctions. *Nat. Cell Biol.* 2014;**16** (6): 587-594. doi: 10.1038/ncb2973.

15. Maître J-L, Berthoumieux H, Krens SFG, Salbreux G, Jülicher F, Paluch E, Heisenberg C-P. Adhesion Functions in Cell Sorting by Mechanically Coupling the Cortices of Adhering Cells. *Science* 2012;**338** (6104): 253-256. doi: 10.1126/science.1225399.

16. Murrell MP, Gardel ML. F-actin buckling coordinates contractility and severing in a biomimetic actomyosin cortex. *Proc. Natl. Acad. Sci.* 2012;**109** (51): 20820-5. doi: 10.1073/pnas.

17. Carvalho K, Tsai FC, Lees E, Voituriez R, Koenderink GH, Sykes C. Cell-sized liposomes reveal how actomyosin cortical tension drives shape change. *Proc. Natl. Acad. Sci.* 2013; **110** (41): 16456-61. doi: 10.1073/pnas.1221524110.

18. Carvalho K, Lemière J, Faqir F, Manzi J, Blanchoin L, Plastino J, Betz T, Sykes C. Actin polymerization or myosin contraction: two ways to build up cortical tension for symmetry breaking. *Philos. Trans. R. Soc. B Biol. Sci.* 2013;**368** (1629):20130005. doi: 10.1098/rstb.2013.0005.

19. Ramachandran A, Anderson TH, Leal LG, Israelachvili JN. Adhesive interactions between vesicles in the strong adhesion limit. *Langmuir*. 2011; 27(1): 59–73. doi:10.1021/la1023168.

20. van der Gucht J, Paluch E, Plastino J, Sykes C. Stress release drives symmetry breaking for actin-based movement. *Proc. Natl. Acad. Sci.* 2005;**102** (22): 7847-7852.

21. Kawska A, Carvalho K, Manzi J, Boujemaa-Paterski R, Blanchoin L, Martiel J-L, Sykes C. How actin network dynamics control the onset of actin-based motility. *Proc. Natl Acad. Sci*. 2012;**109** (14): 440-445. doi:10.1073/pnas.1117096109.

22. Noireaux V, Golsteyn RM, Friederich E, Prost J, Antony C, Louvard D, Sykes C. Growing an Actin Gel on Spherical Surfaces. Biophys.J. 2000; **78:** 1643–1654.

23. Betz T and Sykes C. Time resolved membrane fluctuation spectroscopy. *Soft Matter* 2012; **8**: 5317-5326. DOI: 10.1039/c2sm00001f.

24. Faucon JF, Mitov MD, Méléard P, Bivas I, Bothorel P. Bending elasticity and thermal fluctuations of lipid membranes. Theoretical and experimental requirements. *J. Phys. France* 1989; **50**: 2389-2414.

25. Pecreaux J, Dobereiner H-G, Prost J, Joanny J-F, Bassereau P. Refined contour analysis of giant unilamellar vesicles. *Eur. Phys. J. E Soft Matter* 2004;**13** (3): 277-290.

26. Monzel C, Schmidt D, Kleusch C, Kirchenbüchler D, Seifert U., Smith A-S, Sengupta K., Merkel R. Measuring fast stochastic displacements of bio-membranes with dynamic optical displacement spectroscopy. *Nat Commun* 2015; 6: 8162.

27. Kunda P, Pelling AE, Liu T, Baum B. Moesin controls cortical rigidity, cell rounding, and spindle morphogenesis during mitosis. *Curr. Biol. CB*. 2008; **18** (2): 91-101. doi: 10.1016/j.cub.2007.12.051.

28. Marcy Y, Prost J, Carlier M-F, Sykes C. Forces generated during actin-based propulsion: direct measurement by micromanipulation. *Proc Natl Acad Sci USA* 2004; **101**(16): 5992–5997.

29. Harris DE, Warshaw DM. Smooth and skeletal muscle myosin both exhibit low duty cycles at zero load in vitro. *J. Biol.Chem*. 1993; **268**(20):14764-14768.
30. Finer JT, Simmons RM, Spudich JA. Single myosin molecule mechanics: Pico- newton forces and nanometre steps. *Nature* 1994; **368**(6467):113-119.
31. Backouche F, Haviv L, Groswasser D, Bernheim-Groswasser A. Active gels: dynamics of patterning and self-organization. *Phys. Biol.* 2006; **3**: 264–273.
32. Bendix PM, Koenderink GH, Cuvelier D, Dogic Z, Koeleman BN, Brieher WM, Field CM, Mahadevan L, Weitz DA. A Quantitative Analysis of Contractility in Active Cytoskeletal Protein Networks. Biophys. J. 2008; **94**: 3126–3136.
33. Murrell M, Gardel ML. Actomyosin sliding is attenuated in contractile biomimetic cortices. MBoC 2014; **25**: 1845-1853.
34. Köster DV, Husain K, Iljazi E, Bhat A, Bieling P, Mullins RD, Rao M, Mayor S. Actomyosin dynamics drive local membrane component organization in an in vitro active composite layer. PNAS 2016; E1645–E1654.
35. Chaigne, A., Campillo, C., Gov, N. S., Voituriez, R., Sykes, C.,Verlhac, M. H., & Terret, M. E. A narrow window of cortical tension guides asymmetric spindle positioning in the mouse oocyte. *Nature Communications*, 2015; **6**, 6027. doi:10.1038/ncomms7027.
36. Fritzsche M, Erlenkämper C, Moeendarbary E, Charras G, Kruse K. Actin kinetics shapes cortical network structure and mechanics. *Sci. Adv*. 2016;2:e1501337.
37. Takiguchi K. Yamada A, Negishi M, Tanaka-Takiguvhi Y, Yoshikawa K. *Langmuir* 2008; 24 (20): 11323-11326.
38. Tsai F, Stuhrmann B, Koenderink GH. Encapsulation of Active Cytoskeletal Protein Networks in Cell-Sized Liposomes. *Langmuir* 2011; 27 (16): 10061–10071.
39. Abu Shah E, Keren K. Symmetry breaking in reconstituted actin cortices. *eLife* 2014; **3:** e01433. doi: 10.7554/eLife.01433.
40. Loiseau E, Schneider J.A.M, Keber F.C, Pelzl C,Massiera G, Salbreux G, Bausch A.R. Shape remodeling and blebbing of active cytoskeletal vesicles. *Sci. Adv.* 2016; 2 (4):e1500465.
41. Pontani L-L, van der Gucht J, Salbreux G, Heuvingh J, Joanny J-F, Sykes C. Reconstitution of an Actin Cortex Inside a Liposome. *Biophys. J.* 2009; **96**:192-198.
42. Koenderink GH, Dogic Z, Nakamura F, Bendix PM, MacKintosh FC, Hartwig JH, Stossel TP, Weitz DA. An active biopolymer network controlled by molecular motors. *Proc. Natl. Acad. Sci.* 2009; **106** (36): 15192-15197. doi: 10.1073/pnas.0903974106.
43. Toyoshima YY, Kron SJ, McNally EM, Niebling KR, Toyoshima C, Spudich JA. Myosin subfragment-1 is sufficient to move actin filaments in vitro. *Nature* 1987; **328** (6130): 536-539.
44. Angelova M, Dimitrov D. Liposome electroformation. *Faraday Discuss.* 1986; **81:** 303-311.
45. Lemière J, Carvalho K, Sykes C Cell-sized liposomes that mimic cell motility and the cell cortex. *Methods Cell Biol.* 2015; **128**: 271-85.

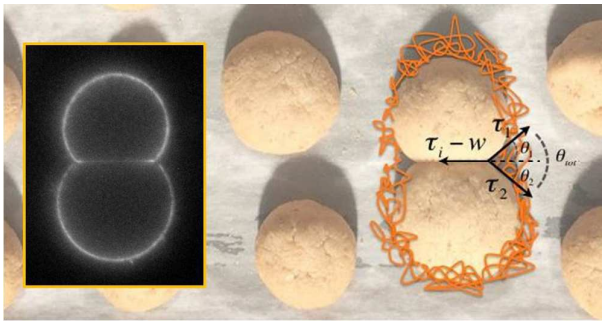

Quantitative measurements of tension generated by an artificial actomyosin cortex reconstituted at the outer surface of liposome doublets, as sweetly schematized by halves of Italian cookies “baci di dama” that happen to stick.